Asymmetric High-Velocity Ejecta in the Youngest Galactic Supernova Remnant G1.9+0.3

Kazimierz Borkowski, Stephen Reynolds (North Carolina State University), David Green (Cambridge University),
Una Hwang (University of Maryland), Robert Petre (NASA/Goddard Space Flight Center), Rebecca Willett (University of Wisconsin-Madison),
Heather Johnson (University of Texas), John Blondin, Carla Fröhlich (North Carolina State University)

G1.9+0.3: The Youngest Galactic SNR

- About 100 yr old from global expansion measurements (Carlton et al. 2011)
- 2 pc in size at the Galactic center distance of 8.5 kpc
- X-ray spectrum dominated by synchrotron emission; highly absorbed ($N_H \sim 6 \times 10^{22}$ cm^{-2})
- Most likely the result of an asymmetric Type Ia supernova explosion (Reynolds et al. 2008; Borkowski et al. 2013b)

  18,000 km/s free expansion velocities
  No pulsar-wind nebula (but any neutron star/CCO would be hidden by high absorption)
  Bilaterally symmetric X-ray synchrotron: like SN 1006

Supernova Ejecta

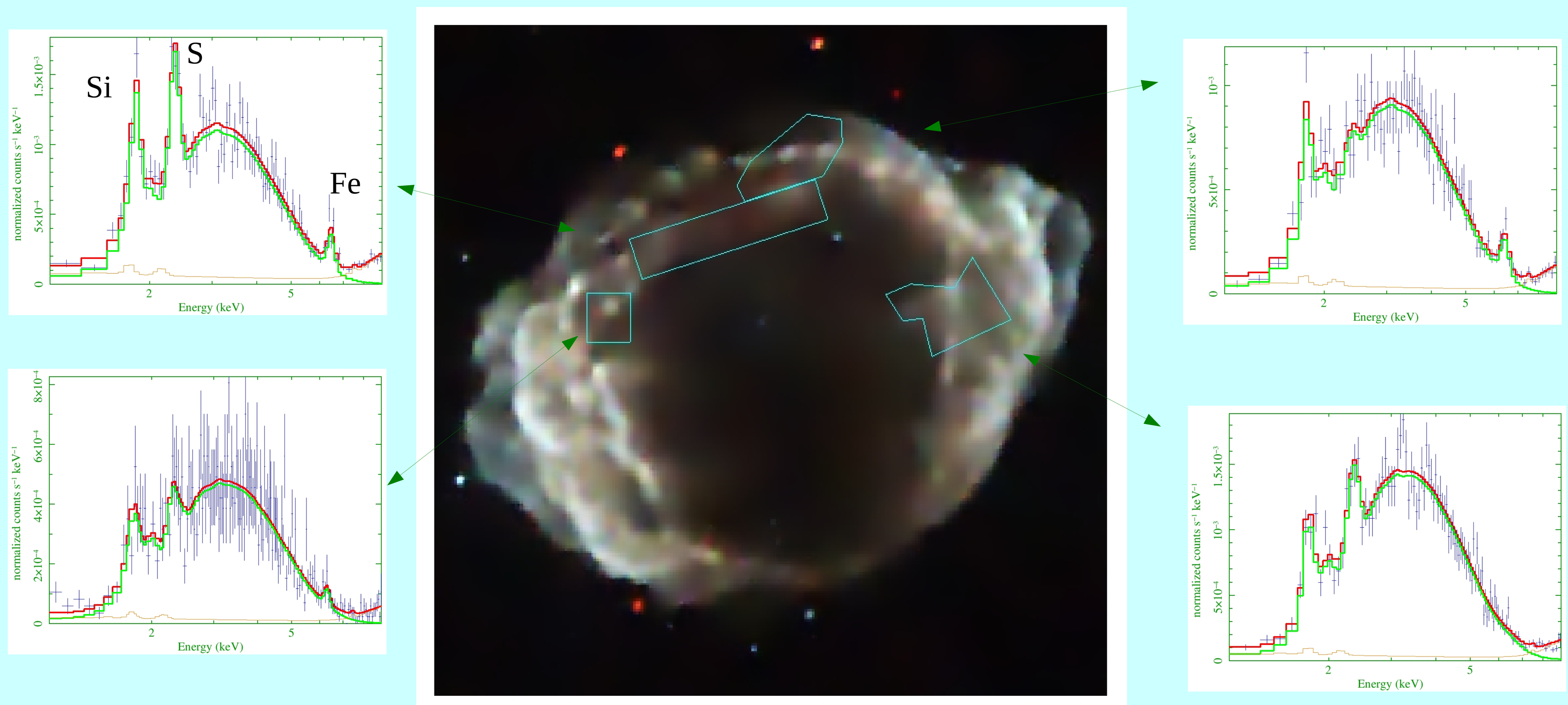

A composite G1.9+0.3 X-ray image: soft (1-3 keV) X-rays in red, medium (3-4.5 keV) X-rays in green, and hard (4.5-7.5 keV) X-rays in blue. X-ray images have been extracted from a Chandra datacube smoothed (denoised) with a spatio-spectral method of Krishnamurthy, Raginsky & Willett (2010). Spectral lines seen in spectra come from **freshly-synthesized Fe and freshly-synthesized intermediate-mass (Si and S) elements (IMEs)**.

Type Ia Explosions with Very High-Velocity ^{56}Ni

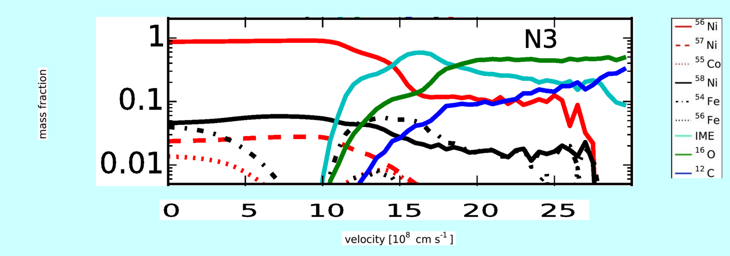

An energetic 3D **delayed detonation Type Ia model** from Seitenzahl et al. (2013). Chemical abundances vs. free-expansion velocity (averaged over angles). **Radioactive ^{56}Ni extends to very high (>20,000 km/s) velocities**, matching spectra of Type Ia supernovae such as SN 2010jn (Hachinger et al. 2013). Spatial distributions of ^{56}Ni and intermediate-mass elements are very asymmetric in this model. Since only high-velocity Fe has been shocked so far in G1.9+0.3, this remnant may have been produced by such an asymmetric and energetic Type Ia explosion. **4.4 x 10^{-6} solar masses of ^{44}Ti was synthesized in N3 model, comparable with 1 x 10^{-5} solar masses implied by a possible detection of the 4.1 keV ^{44}Sc line in the interior of G1.9+0.3.**

Nonuniform Expansion

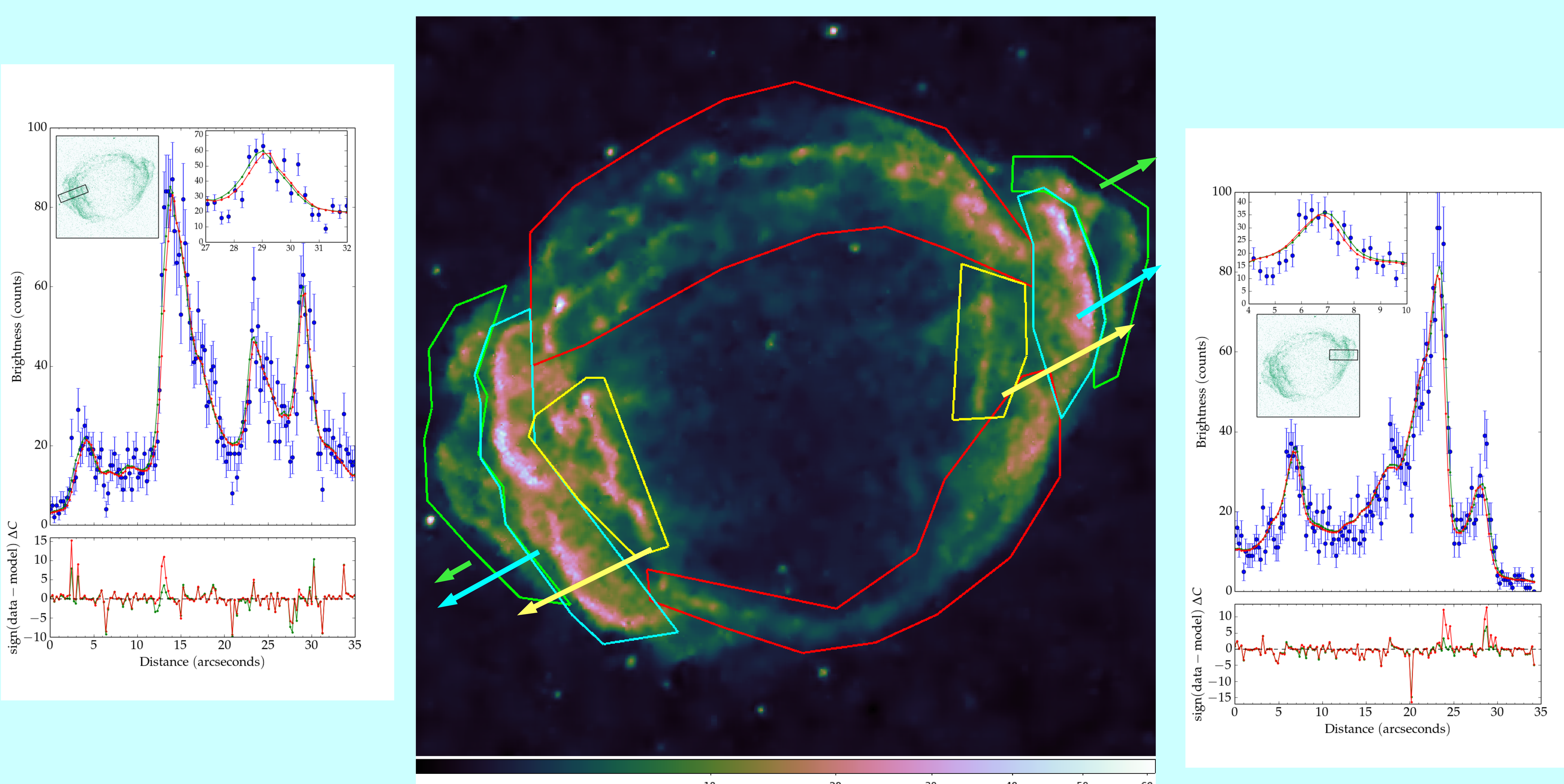

Profile of SE limb. Blue: 2009 data. Red: fit to inner rim by shrinking 2011 data by 0.84%/yr. Green: fit to bright rim by shrinking by 0.62%/yr. Inset: blowup of inner rim. Fit to inner rim shrinks too much for bright rim. Fit to bright rim shrinks too little for inner rim.

2011 image, smoothed with multiscale partitioning method of Krishnamurthy et al. (2010). Scale: counts/ACIS pixel between 1.5 and 8 keV. Pairs of regions used for expansion measurements are shown (inner rims: yellow, middle rims: cyan, ears: green, N-S rims: red). Schematic of relative expansion rates of three pairs of regions indicated by arrows (rates not to scale). Intensities shown with cubehelix color scheme of Green (2011).

Profile of NW limb. Blue: 2009 data. Red: fit to inner rim by shrinking 2011 data by 0.84%/yr. Green: fit to bright rim by shrinking by 0.62%/yr. Inset: blowup of inner rim. Fit to inner rim shrinks too much for bright rim. Fit to bright rim shrinks too little for inner rim.

Asymmetric Radio Emission

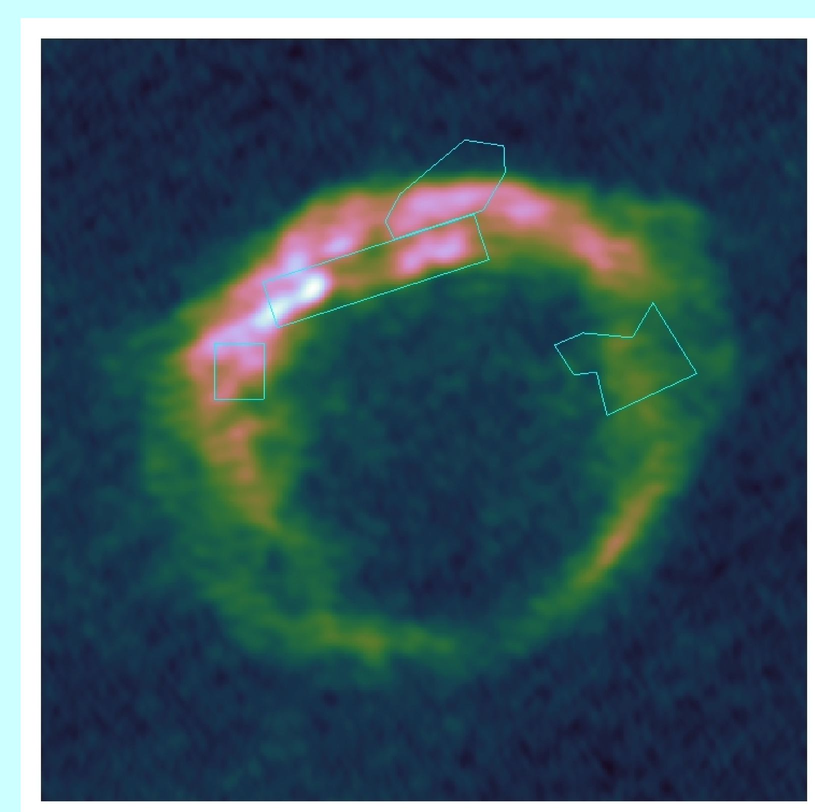

1.4 GHz VLA image from 2008 December. The bright northern shell dominates, while prominent hard X-ray protrusions ("ears") in the NW and SE are very faint in radio. Bright radio emission correlates with ejecta emission, particularly with Fe. Intensities shown with cubehelix color scheme of Green (2011).

Hydrodynamical Simulations

- Simulations in 3D using VH-1 hydrocode on an expanding 512^3 Cartesian grid
- Initial conditions: N3 model in free expansion from Seitenzahl et al. (2013), expanding into uniform ambient medium with hydrogen density 0.014 cm^{-3}
- Ejecta kinetic energy: 1.6x10^{51} ergs, ejecta mass: 1.4 solar masses, mass of iron: 1.1 solar, intermediate-mass elements (IMEs): 0.12 solar

Simulated Remnant at 100 yr

- Shocked ISM mass (in solar masses): 0.016, O: 0.015 (35% of total), IMEs: 0.022, Fe-group elements (mostly Fe): 0.015
- Amounts of shocked Fe and IMEs are sufficient to account for strengths of Si, S, and Fe lines detected in G1.9+0.3
- Remnant appears only mildly (20%) aspherical, but its center is displaced by about 20% from the true explosion center

Expansion Measurements

Data: *Chandra* ACIS-S3. 50 ks (2007, Epoch I); 237 ks (2009, Epoch II; 2.413 yr later); 977 ks (2011, Epoch III; 4.274 yr later).

Method as in Carlton et al. 2011: Smooth 2011 datacube with method of Krishnamurthy et al. (2010) ("model"; 1.2 – 8 keV). Background subtract; shrink to fit Epoch I and II images with 4-parameter fit: expansion rate, brightness change, expansion center coordinates.

Overall expansion (entire remnant): 0.589 ± 0.016%/yr (consistent with Carlton et al. 2011).

Repeat for 4 pairs of opposing regions: 3 pairs along SE-NW (inner rims, bright rims, ears); one SW-NE.

Three pairs of structures perpendicular to SE-NW axis: we assume
- inner rims: reverse shock
- bright rims: majority of blast wave
- outermost emission ("ears"): faster ejecta seen in projection (?)

Rates: Ears, 0.52 ± 0.03%/yr; bright rims, 0.616 ± 0.024%/yr; inner rims, 0.84 ± 0.06%/yr. N-S: 0.576 ± 0.32%/yr.

Overall brightness change: Increase by 1.9 ± 0.4%/yr.

Images of Simulated Remnant at 100 yr

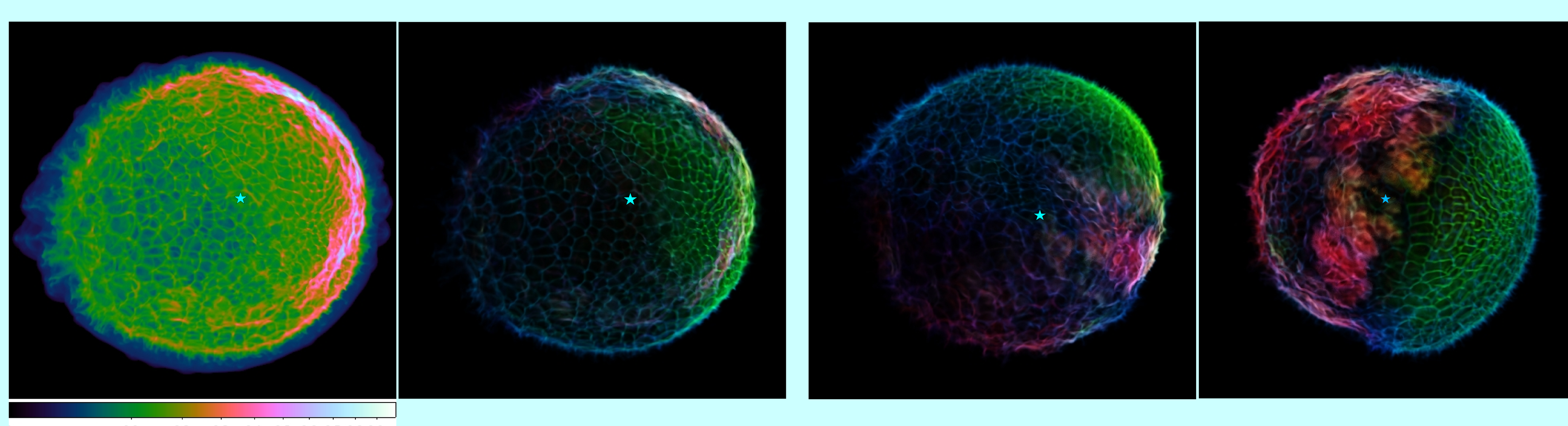

View of the simulated remnant along the line of sight perpendicular to the major axis. Star marks the explosion site. Left: Normalized "emission measure" (integral of density squared along the line of sight) of shocked gas. Right: Emission measures for O (blue), IMEs (green), and Fe-group elements (red). **There is a large contrast in the limb brightness between opposing hemispheres**, with the much higher intensity closer to the explosion site.

Left: Another view along the minor axis (rotated by 90° relative to the previous view). Right: Pole-on view. **Iron (red) is very asymmetrically distributed.** It is localized mostly in regions where the deflagration ashes have risen to the surface of the white dwarf prior to its final detonation. IMEs (green) are more uniformly distributed.

Expansion Rate and Brightness Increase

Measured expansion rates **strongly deviate from uniform expansion**, increasing inward by about 60% along the X-ray bright SE-NW axis.

Corresponds to undecelerated ages of 120 – 190 yr, confirming the young age of G1.9+0.3, and implying **significant (deceleration parameter m < 0.6) deceleration of the blast wave.**

Spatially-integrated X-ray flux, strongly dominated by synchrotron emission, **increases at a rate of 1.9% ± 0.4% per year**, in agreement with previous measurements.

The radio flux is rising at 1%-2% per year (Green et al. 2008; Murphy et al. 2008).

G1.9+0.3 is the only Galactic SNR increasing in brightness at X-ray and radio wavelengths.

Conclusions

1. **Expansion: Structure in density, either in the ejecta or the surrounding medium, is required to produce the greater deceleration at larger radii.**
2. **Expansion: Some supernova models, including pulsating delayed-detonation models, naturally produce qualitative features of the kind required, but disagree quantitatively (Borkowski et al. 2014).**
3. **Ia Models: 3D models of energetic Type Ia explosions can explain strong asymmetry and presence of shocked Fe and IMEs: N3 model of Seitenzahl et al. (2013) provides the best match.**
4. **Simulations: Preliminary results predict shocked masses consistent with the observed line strengths, and indicate a much more asymmetric distribution of Fe compared to IMEs.**

References

Borkowski, K.J., et al. 2013a, BAAS, 13, 127.06 (possible detection of the ^{44}Sc line)
Borkowski, K.J., et al. 2013b, ApJ, 771:L9
Borkowski, K.J., et al. 2014, ApJ, 790:L18 (nonuniform expansion)
Carlton, A.K., et al. 2011, ApJ, 737, L22
Green, D.A., et al. 2008, MNRAS, 387, L54
Green, D.A. 2011, Bull.Astr.Soc.India, 39, 289
Hachinger, S., et al. 2013, MNRAS, 429, 2228
Krishnamurthy, K., et al. 2010, SIAM J. Imaging Sci., 3, 619
Murphy, T., et al. 2008, MNRAS, 389, 23
Reynolds, S.P., et al. 2008, ApJ, 680, L41
Seitenzahl, I., et al. 2013, MNRAS, 429, 1156 (see also Erratum in MNRAS, 444, 350)

This work is based on Chandra data. We acknowledge support from NASA awards SAO G01-12098A and B. H.J. was supported by NSF grant for Undergraduate Research in Computational Astrophysics at NCSU.

URCA
Undergraduate Research in Computational Astrophysics